NEOPLASIA
www.neoplasia.com

Volume 21 Number 10 October 2019 pp. 974–988 974

Targeting c-MYC through Interference with NAMPT and SIRT1 and Their Association to Oncogenic Drivers in Murine Serrated Intestinal Tumorigenesis[1]

Lydia Brandl[*,2], Yina Zhang[*,†,‡,2], Nina Kirstein[*,†,3], Andrea Sendelhofert[*], Sophie Luise Boos[*,‡], Peter Jung[*,‡], Florian Greten[§], Roland Rad[¶] and Antje Menssen[*,†,‡]

*Institute of Pathology, Ludwig-Maximilians University (LMU), Thalkirchnerstraße 36, 80337 Munich, Germany; †Research group "Signaling pathways in colorectal cancer"; ‡German Cancer Consortium (DKTK), and German Cancer Research Center DKFZ, Im Neuenheimer Feld 280, 69120 Heidelberg, Germany; §Institute for Tumor Biology and Experimental Therapy, Georg-Speyer-Haus, Paul-Ehrlich-Straße 42-44, 60596 Frankfurt/Main, Germany; Frankfurt Cancer Institute, Goethe University Frankfurt, 60596 Frankfurt/Main, Germany;and German Cancer Consortium (DKTK) and German Cancer Research Center DKFZ, Im Neuenheimer Feld 280, 69120 Heidelberg, Germany; ¶Institute of Molecular Oncology and Functional Genomics, School of Medicine, Technical University of Munich, Munich, Germany; Center for Translational Cancer Research (TranslaTUM), Technical University of Munich, Germany; Department of Medicine II, School of Medicine, Technical University of Munich, Germany; German Cancer Consortium (DKTK) and German Cancer Research Center (DKFZ), Im Neuenheimer Feld 280, 69120 Heidelberg, Germany

Abstract

We recently described a positive feedback loop connecting c-MYC, NAMPT, DBC1 and SIRT1 that contributes to unrestricted cancer cell proliferation. Here we determine the relevance of the loop for serrated route intestinal tumorigenesis using genetically well-defined $Braf^{V600E}$ and $K\text{-}ras^{G12D}$ mouse models. In both models we show that c-MYC and SIRT1 protein expression increased through progression from hyperplasia to invasive carcinomas and metastases. It correlated with high NAMPT expression and was directly associated to activation of the oncogenic drivers. Assessing functional and molecular consequences of pharmacological interference with factors of the loop, we found that inhibition of NAMPT resulted in apoptosis and reduced clonogenic growth in human *BRAF*-mutant colorectal cancer cell lines and patient-derived tumoroids. Blocking SIRT1 activity was only effective when combined with a PI3K inhibitor, whereas the latter antagonized the effects of NAMPT inhibition. Interfering with the positive feedback loop was associated with down-regulation of c-MYC and temporary de-repression of TP53,

Abbreviations: CCAR2, cell cycle and apoptosis regulator 2; CRC, colorectal carcinoma; DBC1, deleted in breast cancer 1; FFPE, formalin-fixed paraffin-embedded; FOXO, forkhead box O; HTOM, human tumor organoid media; IHC, immunohistochemical; mSA-HGD, murine serrated adenomas with high-grade dysplasia; mSA-LGD, murine serrated adenomas with low-grade dysplasia; mSA, murine serrated adenomas; mSH, murine serrated hyperplasia; MSI, microsatellite instable; MSS, microsatellite stable; NAMPT, nicotinamide phosphoribosyltransferase; PARP-1, Poly (ADP-ribose) polymerase 1; PBEF, pre-B cell enhancing factor; PDO, patient derived organoid; PI, propidium iodide; PI3K, phosphatidylinositol 3-kinase; SIRT1, sirtuin-1.

Address all correspondence to: Antje Menssen, Institute of Biochemistry and Molecular Biology, Medical School, RWTH Aachen, Pauwelsstrasse 30, 52074 Aachen, Germany. E-mails: menssenantje@gmail.com, amenssen@ukaachen.de

[1] Declarations of interest: none
[2] equal contribution
[3] present address: Department of Human Genetics, Sylvester Comprehensive Cancer Center, Miller School of Medicine, University of Miami, 1501 NW 10th Avenue, Miami, FL 33136, USA
[4] present address: Institute of Biochemistry and Molecular Biology, Medical School, RWTH Aachen, Pauwelsstrasse 30, 52,074 Aachen, Germany

Received 23 April 2019; Revised 23 July 2019; Accepted 23 July 2019

1476-5586
https://doi.org/10.1016/j.neo.2019.07.009

explaining the anti-proliferative and pro-apoptotic effects. In conclusion we show that the c-MYC-NAMPT-DBC1-SIRT1 positive feedback loop contributes to murine serrated tumor progression. Targeting the feedback loop exerted a unique, dual therapeutic effect of oncoprotein inhibition and tumor suppressor activation. It may therefore represent a promissing target for serrated colorectal cancer, and presumably for other cancer types with deregulated c-MYC.

Neoplasia (2019) 21, 974–988

Introduction

Besides the classical route to colorectal carcinomas (CRC), an alternative, serrated route in the development of colorectal tumors exists which comprises 15% of all CRCs [1–3]. It is characterized by lesions with "saw-tooth" crypt architecture like hyperplastic polyps, sessile serrated adenoma, traditional serrated adenoma and invasive serrated adenocarcinoma [2]. Serrated lesions have either *BRAF* (80%) or *KRAS* (20%) mutations. Clinicopathologically, *BRAF*-mutant tumors represent less than 10% of metastatic CRCs. They are associated with a worse prognosis than *BRAF* wild-type tumors [4,5]. Of the *BRAF*-mutant tumors, the most aggressive molecular subtypes are mismatch repair proficient, microsatellite stable (MSS), and usually harbor *TP53* mutations [6]. Although these tumors initially respond better to therapy, the prognosis of patients is very poor, with a median survival of 10 months, compared to 35 months for patients with *BRAF* wild-type tumors [5,7].

Successful generation of *in vivo* models for the serrated route allowed to comprehensively study defining hallmarks in the development of serrated lesions. Conditional *Vil-Cre;Braf*$^{LSL\text{-}V637E/+}$ (which corresponds to human BRAF^{V600E}) and *Vil-Cre,LSL-K-ras*$^{G12D/+}$*/Ink4a/Arf*$^{-/-}$ knock-in mouse models develop murine serrated hyperplasia (mSH), murine serrated adenomas (mSA) and invasive carcinomas in the intestine [8,9], confirming observations made on serrated route lesions of patients. Both models provide functional evidence for the tumor initiating potential of mutant, constitutively active Braf and K-Ras proteins.

We recently described a positive feedback loop connecting the oncoprotein c-MYC, the NAD^+ generating metabolic enzyme nicotinamide phosphoribosyltransferase (NAMPT), the NAD^+-dependent protein deacetylase sirtuin-1 (SIRT1), and the SIRT1 inhibitor deleted in breast cancer 1 (DBC1) (also called cell cycle and apoptosis regulator protein 2 (CCAR2)). Activation of the c-MYC-NAMPT-DBC1-SIRT1 loop contributes to proliferation and survival of cancer cells [10], reviewed in [11]. Our subsequent *in situ* studies confirmed the functional link between c-MYC, NAMPT and SIRT1 as their high expression is correlated in various types of adenomas and tumors [10,12–14]. Importantly, c-MYC is also a major target of WNT signaling which is upregulated early in the conventional pathway of colorectal carcinogenesis [15]. As we have shown before, deregulated c-MYC is associated with high SIRT1 levels in classical adenomas and carcinomas [10,14].

In the serrated route, elevated expression of c-MYC and SIRT1 is linked to the presence of *KRAS* and *BRAF* mutations and strongly associated with higher grades of malignancy [12]. Since SIRT1 inhibits pro-apoptotic factors such as TP53 by deacetylation [16,17], SIRT1 activity antagonizes apoptosis and senescence. Therefore, constitutive activation of this positive feedback loop can contribute to the development and maintenance of tumors.

However, some evidence from *in situ* and *in vivo* studies also point to potential tumor-suppressive functions of SIRT1 [18]. SIRT1 is therefore considered a double-edged sword that has several tumor promoter and suppressor functions depending on the tissue and context. In particular, although the role of SIRT1 in cancer is still unclear, NAMPT and SIRT1 activity enhancers are currently investigated for their potential to extend healthspan and prolong lifespan in humans [19–21].

In view of this, the role of SIRT1 and its upstream regulator NAMPT in tumors should be conclusively clarified at first.

We analyzed c-MYC, NAMPT, DBC1, and SIRT1 expression in genetically well-defined *Braf*^{V637E} and *K-ras*^{G12Dint}*/Ink4a/Arf*$^{-/-}$ mouse models to determine whether activation of c-MYC and its downstream components of the feedback loop are directly linked to the initiating *Braf* and *K-ras* mutations and required for the development of serrated lesions. Additionally, we assessed the impact of NAMPT and SIRT1 inhibition in

Table 1. Number of Investigated Serrated Lesions in *Braf* and *K-Ras* Mutant Mice

Histology	*Vil-Cre; Braf*$^{LSL\text{-}V637E}$	*Vil-Cre; Braf*$^{LSL\text{-}V637E}$*;p16*^{Ink4a}	*Vil-Cre; Braf*$^{LSL\text{-}V637E}$*;p53*$^{LSL\text{-}R172H/+}$	*Vil-Cre; LSL-K-ras*^{G12D}*/ Ink4a/Arf*$^{-/-}$
mSH	5/5 Mice	15/15 Mice	8/8 Mice	14/14 Mice
mSA-LGD	7/5 Mice	9/7 Mice	8/3 Mice	1/1 Mouse
mSA-HGD	23/4 Mice	36/11 Mice	18/6 Mice	1/1 Mouse
Invasive carcinomas	2/2 Mice	12/9 Mice	1/1 Mouse	1/1 Mouse
Lung metastases	–	4/2 Mice	2/1 Mouse	–
Lymph node metastases	–	3/2 Mice	2/1 Mouse	–
Fat tissue metastases	–	1/1 Mouse	–	–
Liver metastases	–	11/2 Mice	–	–

mSH murine serrated hyperplasia; mSA-LGD murine serrated adenoma low-grade dysplasia; mSA-HGD murine serrated adenoma high-grade dysplasia.

Table 2. List of Antibodies and IHC Conditions

	MYC	SIRT1	NAMPT	DBC1
Antibody	Polyclonal rabbit	Polyclonal rabbit	Polyclonal rabbit	Monoclonal rabbit
Company	Millipore, Massachusetts, USA	Atlas antibodies, Stockholm, Sweden	Atlas antibodies, Stockholm, Sweden	Abcam, Cambridge, United Kingdom
Dilution	1:300	1:180	1:200	1:150
Cat. No.	06–340	HPA006295	HPA047776	ab84384
Incubation	Target Retrieval Solution pH 6, Dako, Cat. No. S1699	Target Retrieval Solution Citrate pH 6, Dako, Cat. No. S2369	Pro Taqs II Antigen-Enhancer pH 9.5, Quartett, Cat. No. 401602192	Target Retrieval Solution Citrate pH 6, Dako, Cat. No. S2369
Detection system	ImmPress Reagent Kit Rabbit Ig, Vector Laboratories, Cat. No. MP-7401	ImmPress Reagent Kit Rabbit Ig, Vector Laboratories, Cat. No. MP-7401	ImmPress Reagent Kit Rabbit Ig, Vector Laboratories, Cat. No. MP-7401	ImmPress Reagent Kit Rabbit Ig, Vector Laboratories, Cat. No. MP-7401
Chromogen	DAB+, Dako, Cat. No. K3468	AEC+, Dako, Cat. No. K3469	DAB+, Dako, Cat. No. K3468	DAB+, Dako, Cat. No. K3468

BRAF-mutant human CRC cell lines and patient-derived tumoroids and determined molecular changes following pharmacological disruption of the positive feedback loop. Since the PI3K pathway is commonly altered in CRC [22] and constitutive PI3K signaling is a central mechanism of resistance to various therapies [23], we analyzed short- and long-term effects of combination therapy with a phosphatidylinositol 3-kinase (PI3K) inhibitor.

Materials and Methods

Mouse Tissue

Formalin-fixed paraffin-embedded (FFPE) material from seven control mice, and from mice with the genotypes: *Vil-Cre;Braf*$^{LSL\text{-}V637E}$, *Vil-Cre;Braf*$^{LSL\text{-}V637E}$*;p53*$^{LSL\text{-}R172H/+}$, *Vil-Cre;Braf*$^{LSL\text{-}V637}$*;p16*^{Ink4} [9] and *Vil-Cre;LSL-K-ras*^{G12D}*/Ink4a/Arf*$^{-/-}$ was used [8]. Table 1 provides a summary of murine serrated lesions analyzed in this study comprising normal mucosa, mSH, murine serrated adenomas with low-grade dysplasia (mSA-LGD), murine serrated adenomas with high-grade dysplasia (mSA-HGD), invasive carcinomas and metastases in lymph node, lung, fat tissue and liver. Animal procedures were carried out in compliance with the institutional guidelines of the local government (Regional government of Upper Bavaria).

Immunohistochemistry

Immunohistochemical (IHC) staining was performed on 3 µm consecutive tissue sections of FFPE tumor samples using IHC protocols as detailed in Table 2. All primary antibodies were incubated at room temperature for 1 hour. All slides were counterstained with hematoxylin (Vector Laboratories, CA, USA, Cat. No. H-3401). Staining specificity was evaluated using system controls without primary antibodies, and immunoglobulin isotype control antibodies. Specificity of the SIRT1 and NAMPT antibody was confirmed using *NAMPT* or *SIRT1* siRNA knockdown in cell lines, followed by PFA fixation of cells, embedding and IHC analysis. In addition, NAMPT antibody specificity was validated using mouse tissue in which both *Nampt* alleles had been deleted by Cre recombinase.

Evaluation of c-MYC, NAMPT, SIRT1, and DBC1 Staining

For c-MYC, SIRT1, and DBC1, nuclear expression was evaluated. For NAMPT nuclear and cytoplasmic staining was determined. In normal mucosa and mSH, positive staining confined to the basal third of the crypts in the large intestine or the basal third of villi and crypt in the small intestine was defined as low. Strong was defined as staining from the base to the surface of the crypts, or villi and crypts. In mSA-LGD and mSA-HGD, only areas with intraepithelial neoplasia were considered. In mSA-LGD, mSA-HGD, invasive adenocarcinomas and metastases, the percentage of stained cells was categorized as negative (0%), low (1–30%), moderate (31–70%) and strong (71–100%).

Cell Lines and Reagents

HT29, COLO 205 and COLO 741 cells were provided by Roland Rad (TU Munich). *BRAF*-mutant COLO 741 were initially classified as colorectal cancer cells, but are now considered to derive from a pelvic melanoma metastasis [24]. Therefore, data obtained with COLO 741 are not shown except for immunoblots. HT29 cells were maintained in DMEM (high glucose), RKO cells (kindly provided by Bert Vogelstein) were maintained in MyCoy's 5A modified medium, COLO 741 and COLO 205 cells were kept in RPMI 1640 medium. All media were supplemented with 10% FCS, 1% L-glutamine and 1% penicillin/streptomycin (Invitrogen). FK866 (AdipoGen), sirtinol (Enzo Life Sciences) and the PI3K inhibitor (LY294002 hydrochloride (Tocris)) were dissolved in DMSO and stored at −20 °C. Cells were seeded at a concentration of 0.5×10^4 in 12 well plates. Thirty hours after seeding, FK866, the solvent DMSO, or FK866 combined with LY294002 were added to sub-confluent cells for 72 hours. Sirtinol, the solvent DMSO, or sirtinol combined with LY294002 were added for 48 hours.

3-D Tumoroid Culture

Tumoroids (patient derived tumor organoid 1 (PDTO1) and PDTO2) were derived from two patients undergoing colectomy at the Klinikum Großhadern (LMU Munich). Samples were irreversibly anonymized and work with patient-derived tumor cells has been approved by the LMU ethics commission (project no. 591–16 UE).

Patient-derived tumoroids embedded in matrigel (BD Corning) were cultured in human tumor organoid media (HTOM) consisting of advanced DMEM/F12 media supplemented with 20 mM HEPES and 2 mM glutamax (ThermoFisher Scientific), 1,25 mM n-acetyl cysteine, B27 supplement retinoic acid free (Gibco), 25 ng/ml noggin (Peprotech), 50 ng/ml human recombinant EGF (Peprotech), 7.5 µM SB202190 (Sigma), 0.5 µM galunisertib (LY2157299) (Biozol Diagnostics), 10 nM prostaglandin E2 (Sigma), and 50 µg/ml normocin (Invivogen). For passaging, matrigel and tumoroids were

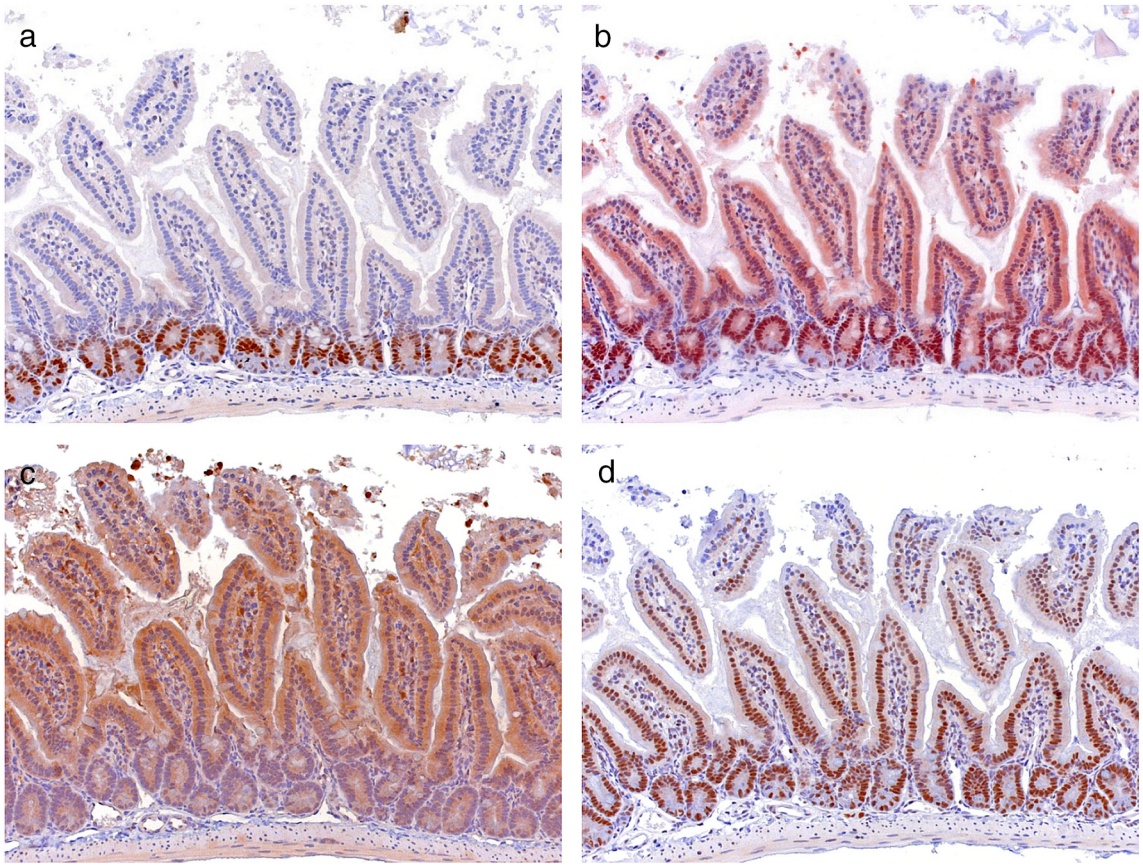

Figure 1. c-MYC and SIRT1 are expressed in the basal third of the crypts, while NAMPT and DBC1 are expressed throughout crypts and villi in normal mucosa of wild-type mice.Immunohistochemical analyses of c-MYC, SIRT1, NAMPT and DBC1 in normal intestinal mucosa of control mice (n = 7). c-MYC (a) and SIRT1 (b) are expressed in the proliferative zone of the crypts. NAMPT is expressed in the cytoplasm of the epithelial cells of the crypts and in the cytoplasm and the nucleus of the villi (c). DBC1 displays homogenous expression along the crypts and villi of the small intestine (d). (Original magnification 200×).

re-suspended in cell recovery solution and incubated on ice for 30 min. Released tumoroids were centrifuged and supernatant was removed. Tumoroids were incubated at 37 °C in 0.025% trypsin/PBS (Gibco). Three thousand disaggregated single cells were plated per 25 µl matrigel in a 48-well plate. Following solidification, HTOM media supplemented with 10 µM Y-27632 (Rock Inhibitor, Biozol Diagnostics) was added and tumoroids were maintained at 37 °C and 5%CO_2.

3-D Tumoroid Drug Treatment and Cell Viability Assessment

Forty-eight hours after tumoroid seeding, sirtinol, FK866, or vehicle control (DMSO) were added to the cultures, respectively. Due to different growth rates, tumoroids were analyzed either 7 days (PDTO1), or 5 days (PDTO2) after addition of the drugs. 3-D cultures were documented with a Nikon AZ-100 macroscope and enhanced focal images were generated with NIS-elements D5.00 software (Nikon).

Viability of tumoroids was determined using the Cell Titer-Glo3D assay (Promega) according to the manufacturer's protocol. Luminescence was measured using a Berthold luminometer (LB96V). All experiments were performed in triplicates.

DNA Content Analysis

Propidium iodide (PI) staining and DNA content analysis was performed as described before [10] using BD Accuri C6 flow cytometer. Experiments were done in biological triplicates and repeated at least twice.

Statistics

Statistics of DNA content analyses were performed in GraphPad Prism 5 using one-way ANOVA followed by Tukey's post-hoc test with alpha = 0.05.

Statistical analyses of two experimental groups of tumoroids was done by t-test, analyses of multiple treatment groups of tumoroids was done by one-way ANOVA with Dunnett's multiple comparisons test.

Long-Term Clonogenic Assay

Cells (3000–6000/ well) were seeded in 6-well plates. Thirty hours after seeding, drugs or DMSO were added once to the cells and plates were sealed using plastic wrap. After 2 weeks, colonies were washed with 1x PBS and fixed with cold methanol (99%) for 30 minutes and stained in 1x modified Giemsa Stain (GS500, Sigma-Aldrich) with gentle rocking (1 hour at room temperature, and 12 hours at 4 ° C). After washing with distilled water, colonies were left to air-dry. Assay conditions were established over a wide range of cell and drug concentrations to obtain cell densities that allowed documentation and quantification. Each drug

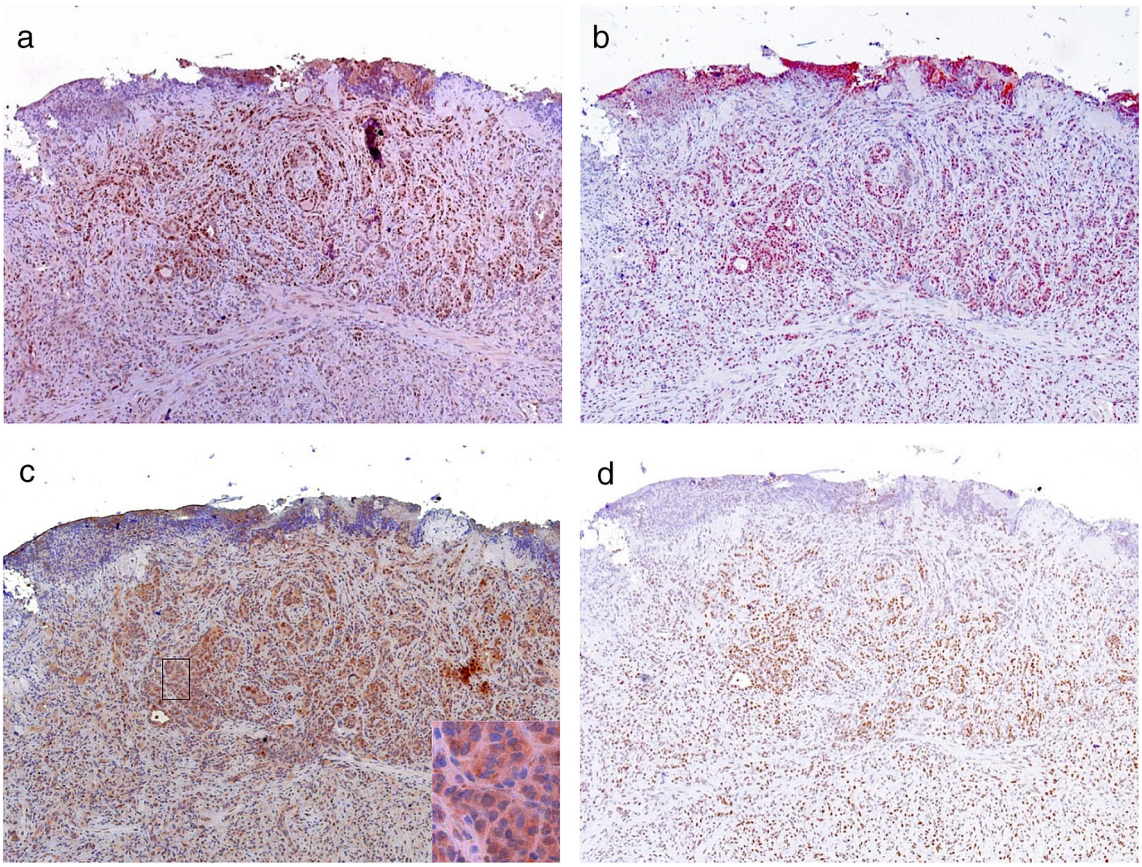

Figure 2. c-MYC, SIRT1, NAMPT and DBC1 are strongly expressed in invasive carcinomas of *Vil-Cre;Braf*$^{LSL\text{-}V637E}$ mice.Expression of c-MYC, SIRT1, NAMPT and DBC1 was analyzed by immunohistochemistry in invasive carcinomas (n = 16). Nuclear c-MYC (a), nuclear SIRT1 (b), cytoplasmic NAMPT (c) and nuclear DBC1 (d) are strongly expressed as more than 70% of the tumor cells reveal a positive staining. Inset shows higher magnification of cytoplasmic NAMPT staining in carcinoma cells. (Original magnification 100×, inset 630×).

concentration was tested at least twice. Colonies were quantified using ImageJ software.

Western Blot Analysis

Immunoblot analysis was done as described before with minor modifications [25]. Cells were harvested at sub-confluence using RIPA buffer and protease inhibitor cocktail (Roche). After sonification, 30–40 µg cell lysate was subjected to electrophoresis. Proteins were blotted on PVDF membranes using Towbin buffer (20% methanol). For detection of c-MYC, SIRT1, p21, NAMPT, TP53 and β-actin antibodies were used as described before [10]. Quantifications of immunoblot signals were done with ImageJ software.

Results

High Expression of c-MYC, NAMPT, DBC1 and SIRT1 in Murine Serrated Intestinal Lesions

To investigate whether the activation of c-MYC and its downstream effectors of the c-MYC/NAMPT/DBC1/SIRT1 feedback loop play a role in the development of serrated lesions, we made use of the *Braf*^{V637E} and *K-ras*^{G12Dint}*/Ink4a/Arf*$^{-/-}$ mouse models. These mouse models develop serrated adenocarcinomas and are characterized by amplified MAPK signaling, while they diverge in other molecular features [8,9]. *Braf*^{V637E} mice progress from hyperplasia to dysplasia, they display *p16*^{Ink4a} and *p19*^{Arf} upregulation, MSI-H, and spontaneous *Tp53* mutations, especially in high-grade dysplasia. Invasive carcinomas develop in a subset of mice and their frequency was considerably increased by the knockin of a mutant *Tp53* gene or *p16*^{Ink4a} inactivation [9]. Kras^{G12Dint} mice develop serrated hyperplasia and lesions are characterized by MSS or MSI-L, the absence of WNT pathway induction, *p16*^{Ink4a} overexpression and oncogene-induced senescence [8]. Overcoming this tumor suppressive mechanism by *Ink4a/Arf* deletion results in more progressed invasive adenocarcinomas in these mice, independent of WNT pathway activation.

We assessed the expression of c-MYC, NAMPT, DBC1 and SIRT1 in progression series of intestinal lesions of 28 *Braf*^{V637E} and 14 *K-ras*^{G12Dint} mice, including *Tp53, p16* and *Arf* mutant compound mice. Table 1 gives a summary of the analyzed mice.

In the mucosa of control mice and in murine serrated hyperplasia (mSH) of all *Braf*^{V637E} and *K-ras*^{G12Dint}, including *Tp53, p16,* and *Arf* compound mice, nuclear c-MYC and SIRT1 expression was restricted to the proliferative zone in the basal third of the crypts in the small (Figure 1, *A* and *B*; Supplemental Figure 1, *A* and *B*) and large intestine. NAMPT was expressed in the cytoplasm of crypt and villus epithelial cells, in the latter partly also in the nucleus (Figure 1*C*; Supplemental Figure 1*C*). Nuclear DBC1 was homogenously expressed along the villi and crypts of the small intestine (Figure 1*D*; Supplemental Figure 1*D*) and crypts of the

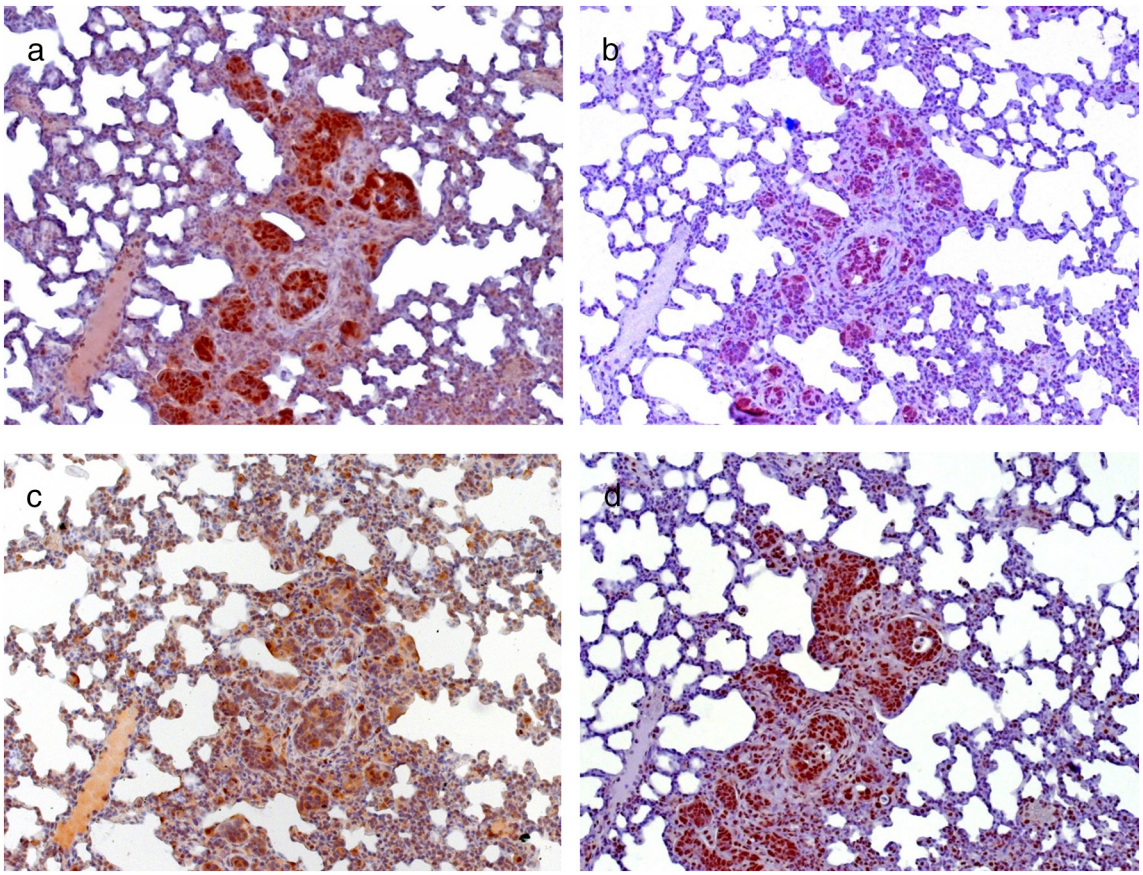

Figure 3. High c-MYC, SIRT1, NAMPT and DBC1 expression in lung metastasis of *Vil-Cre;Braf*$^{LSL\text{-}V637E}$*;p16*^{Ink4a} mice.Immunohistochemical analyses of lung metastasis (n = 4) shows nuclear c-MYC (a), nuclear SIRT1 (b), cytoplasmic NAMPT (c) and nuclear DBC1 (d) are strongly expressed since more than 70% of the tumor cells reveal a positive staining. (Original magnification 200×).

large intestine. In all murine serrated adenomas with low-grade dysplasia (mSA-LGD) and murine serrated adenomas with high-grade dysplasia (mSA-HGD) (Supplemental Figure 2), invasive carcinomas (Figure 2), and metastases (Figure 3) (exemplary for lung) strong nuclear expression of c-MYC, SIRT1 and DBC1, and strong cytoplasmic, but no nuclear NAMPT expression was detected in nearly all cells. These observations were in accordance with upregulation of other effectors downstream of c-MYC in the Braf mouse model, such as *p19*^{Arf} [9]. Unexpectedly, high-grade dysplastic lesion (Supplemental Figure 2) and carcinomas (Figure 2) that are characterized by additional WNT pathway activation did not reveal stronger expression of c-MYC, or other components of the feedback loop.

The concomitant high expression indicated the interconnectedness of c-MYC, NAMPT, and SIRT1 in a positive feedback loop. Its association with the initiating oncogenic drivers pointed to a contribution to tumorigenesis in these mice.

BRAF-Mutant CRC Cell Lines are Sensitive to NAMPT Inhibition

Some molecular subtypes of *BRAF*-mutant CRCs have a poor prognosis and are refractory to therapy. In regard of this unmet medical need, we tested whether NAMPT and SIRT1 may represent therapeutic targets in human serrated colorectal cancer. We used two cell lines, HT29 and COLO 205 that display the combination of genomic alterations (mutant *BRAF,* mutant *TP53,* and microsatellite stability (MSS)) associated with very bad prognosis. Furthermore, we used RKO, a *BRAF*-mutant line with microsatellite instability (MSI) that harbors *TP53* wild-type alleles (according to the COSMIC database at https://cancer.sanger.ac.uk/cell_lines). We assessed DNA content upon short-term drug exposures, and colony growth after 14 days (long-term) in the three cell lines to obtain insight into drug kinetics and mechanisms of drug action.

The three cell lines revealed substantial sensitivity difference upon exposure to the NAMPT inhibitor FK866. COLO 205 CRC cells, which grow partly in suspension, were highly sensitive. Low amounts of FK866 (5 nM) strongly induced apoptosis (70% sub-G_1) (Figure 4*A*) and led to pronounced growth reduction in the clonogenic assay (Figure 4*B*, upper row). FK866 (30 nM) resulted in a nine-fold increased apoptosis rate in HT29 (Figure 4*A*) and clonogenic growth was completely abolished in the presence of 60 nM FK866 (Figure 4*B*, upper row). NAMPT inhibition was ineffective in RKO after 3 days of treatment using up to 150 nM FK866 (Figure 4*A*). In contrast, in the presence of 40 nM FK866 clonogenic growth of RKO cells almost completely stopped after 2 weeks (Figure 4*B*, upper row).

Immunoblot analysis showed that the most sensitive line, COLO 205, expressed the lowest NAMPT levels, whereas HT29 and RKO with high expression were intermediate- or non-responsive

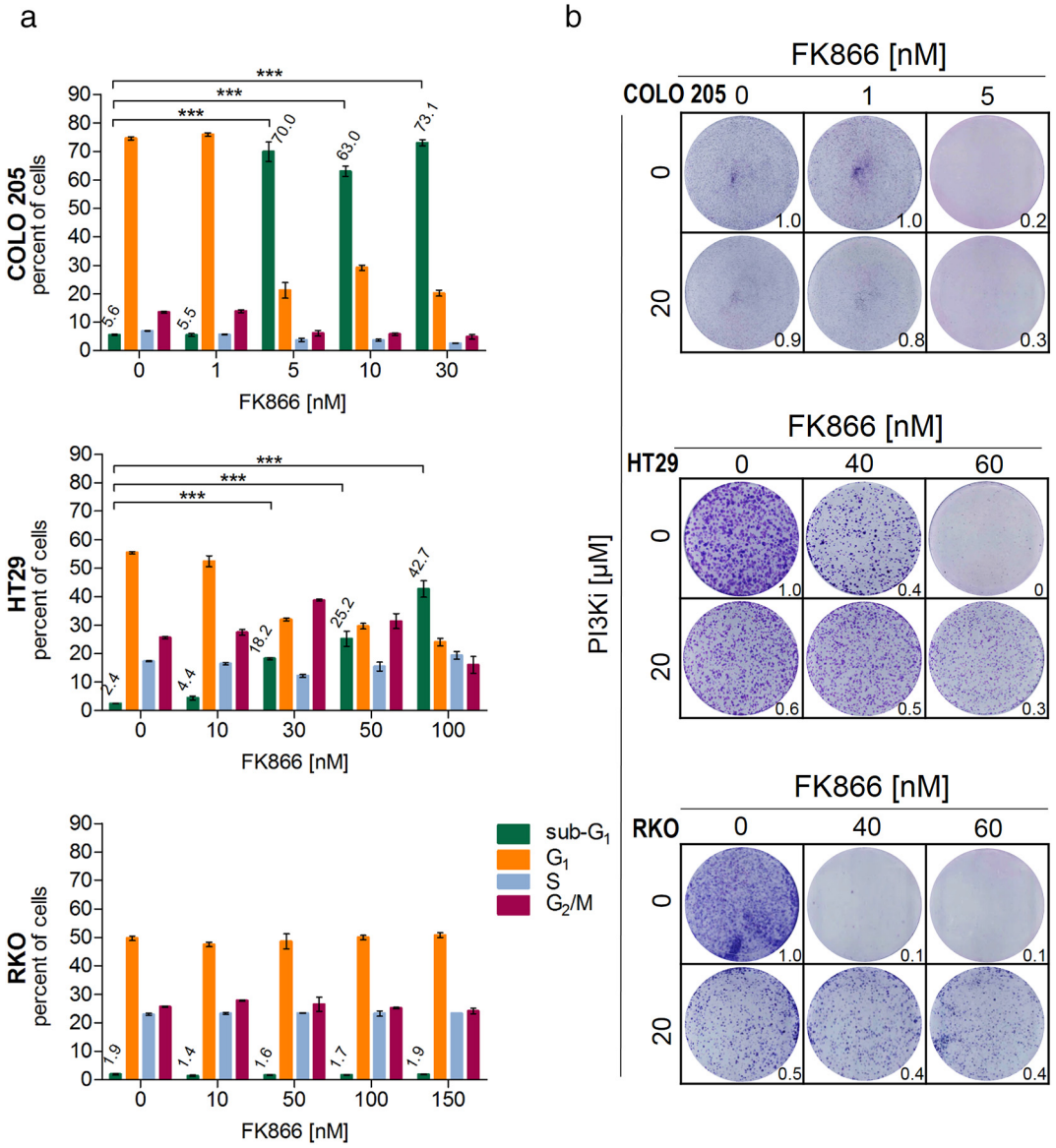

Figure 4. Inhibition of NAMPT by FK866 leads to apoptosis and reduced colony growth while the combination with a PI3K inhibitor has antagonistic effects in *BRAF*-mutant CRC cell lines.(a) The indicated cell lines were exposed to increasing concentrations of the NAMPT inhibitor FK866, or solvent (0) for 3 days. FACS was used to determine DNA content of biological triplicates. Percentages with standard deviation of sub-G_1, G_1, S and G_2/M cell cycle phases are depicted. Percentage values of sub-G_1 fractions are given as indicated. Statistical analysis of one-way ANOVA followed by Tukey's post-hoc test. * $p < .05$, ** $p < .01$, *** $p < .001$.(b) Colony-forming assays document cell viability upon single and combined pharmacological inhibition of NAMPT and PI3K in *BRAF*-mutant human colorectal cancer cell lines. Clonogenic assays were performed after 2 weeks inoculation of FK866, or solvent (0), as single agent (upper row), or its combination with the PI3K inhibitor LY294002 (lower row) at the indicated concentrations. Image J software was used for quantification of Giemsa stained colonies. The area covered by untreated cells was defined as 1. Ratios of inhibitor treated cells *versus* untreated cells are given in the lower right corners.

(Supplemental Figure 3) suggesting that sensitivity to FK866 was inversely correlated with NAMPT protein levels.

Ineffective Monotherapy Using the SIRT1 Inhibitor Sirtinol in BRAF-Mutant CRC Cell Lines

Compared to controls, exposition to the SIRT1 inhibitor sirtinol (70 µM or 100 µM) only slightly induced apoptosis (sub-G_1 population) in COLO 205 (1.6-fold), RKO (4.4-fold) and HT29 (6.6-fold) after two days of drug treatment (Supplemental Figure 4*A*). Sirtinol (70 µM) resulted in a G_1-cell cycle arrest in COLO 205 and HT29 cells. Despite the initial mild apoptosis increase, colony growth was unaffected in all lines (Supplemental Figure 4*B*, upper rows). In contrast, sirtinol strongly abrogated colony growth of the melanoma cell line COLO 741 (that until recently was misidentified as a colorectal cancer cell line) when applied in the same concentration range in a parallel experiment (data not shown).

Immunoblot analysis showed low, intermediate, and high SIRT1 protein expression in COLO 205, HT29 and RKO, respectively (Supplemental Figure 3). The expression inversely correlated with the efficacy of apoptosis induction. Levels of c-MYC protein correlated with NAMPT and SIRT1 in the three CRC cell lines, which was consistent with our previous observation [10]. In line with the role of

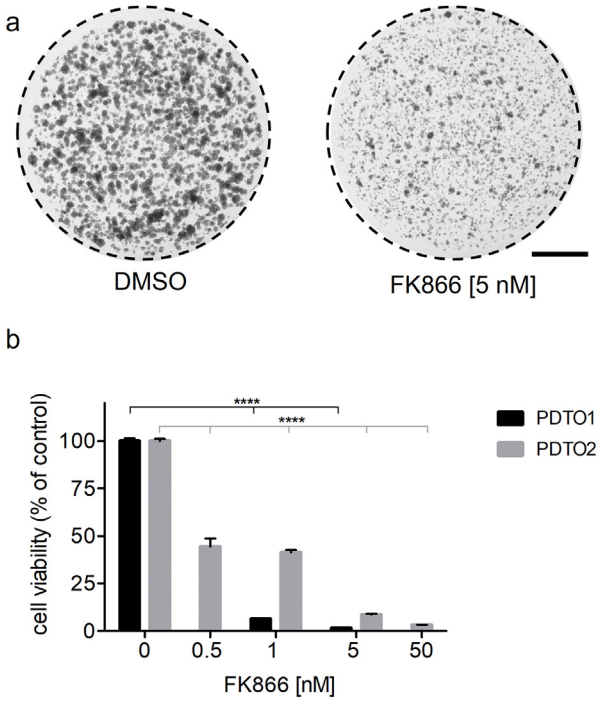

Figure 5. Colony-forming assays demonstrate growth inhibition of patient-derived *BRAF*-mutant human colorectal tumoroids upon NAMPT inhibition.(a) FK866 efficiently inhibits growth of a primary, a *BRAF(V600E)* mutation harboring tumor organoid culture (PDTO2). Single tumoroids plated in 3-D matrigel were inoculated with the indicated concentrations of FK866, or the solvent (DMSO) 48 hours after seeding. Organoid growth was documented *via* enhanced focal imaging microscopy 5 days after treatment. One exemplary image of FK866 treated and DMSO treated tumoroids is depicted. Scale bars represent 1 mm. Dashed lines represent margins of matrigel droplets.(b) Concentration dependent effect on cell viability of tumoroid cultures of two patients (PDTO1 and PDTO2) was assessed *via* indirect luminometric detection of the cellular ATP content (3-D Cell TiterGlo assay). Cell viability was determined relative to the DMSO control (0 nM FK866). Data were obtained from biological triplicates of PDTO1 7 days, and PDTO2 5 days after drug addition, respectively. Error bars indicate standard deviation. Experiments on PDTOs were performed in triplicates. For statistics analyses one-way ANOVA with Dunnett's multiple comparisons test was used. Asterisks indicate statistical significance (****: $p < .0001$).

the PI3K pathway in blocking c-MYC degradation [26], *PIK3CA*-mutant HT29 and RKO lines expressed higher c-MYC levels than COLO 205.

BRAF-Mutant Patient-Derived Colorectal Organoids are Highly Sensitive to NAMPT Inhibition and Insensitive to SIRT1 Inhibition

Next, we tested whether patient derived CRC organoids (PDTOs) displayed similar drug sensitivities as the established CRC cell lines grown in a two-dimensional monolayer. These tumoroids grow in a three-dimensional matrix, which more accurately resembles architecture and behavior of cancer tissues and may lead to different cellular behavior and drug responses [27]. We analyzed NAMPT and SIRT1 inhibition in two $BRAF^{V600E}$-mutant patient derived tumoroids that were microsatellite instable (MSI), while we could not get access to *BRAF*-mutant tumor organoids of the MSS subtype due to the low probability of co-occurrence of *BRAF* mutations and MSS (6.4%, [28]). FK866 treatment had strong growth-inhibitory effects on the 3-D culture of both patients' tumoroids (Figure 5*A*). With 5 or 7 days of treatment, FK866 significantly affected viability of both primary tumor organoids in a concentration-dependent manner (Figure 5*B*). Cell viability was strongly reduced even at low concentrations of 0.5 nM FK866, indicating very high sensitivity of these tumoroids towards NAMPT inhibition. Sirtinol did not show any effect on growth of both tumoroids at 10 μM (Supplemental Figure 5), the maximum applicable concentration. The combination therapy was not assessed in organoids because combining FK866 was not beneficial in all CRC cell lines and sirtinol precipitated at higher concentrations.

Taken together, sirtinol applied as monotherapy in the low micromolar range did not affect growth of CRC cell lines and primary tumoroids. In contrast, all *BRAF*-mutant cell lines, as well as patient-derived tumoroids were highly sensitive to FK866-mediated inhibition of NAMPT activity.

Combination with a PI3K Inhibitor Antagonized Efficacy of NAMPT Inhibition While It Sensitized to SIRT1 Inhibition in BRAF-Mutant CRC Cell Lines

Activating mutations in the genes encoding the PI3K signaling system are common in many human cancers and have been associated with resistance to various targeted therapies [23]. Since HT29 and RKO cell lines harbor mutations in *PIK3CA*, we asked whether concomitant inhibition of PI3K increases sensitivity to NAMPT or SIRT1 inhibitors. We used LY294002, an ATP-competitive and isoform-nonselective PI3K inhibitor and determined concentrations for each cell line that allowed to assess additive effects when given as combination therapy with NAMPT or SIRT1 inhibitors. Addition of LY294002 (40 μM) for 2 days resulted in a sub-G_1 fraction below 20% (Supplemental Figure 6), and less than 30%, when added for 3 days to HT29 and RKO cells (Figure 6*B*). We used 40 μM of LY294002 for the analyses of drug combinations in HT29 and RKO, and due to their higher sensitivity, 20 μM for COLO 205.

Compared to the PI3K inhibitor alone, combined inhibition with the SIRT1 inhibitor collectively resulted in drug synergism as the rate of apoptosis raised 1.7-, 2.5-, and 2.8-fold in RKO, COLO 205, and HT29, respectively (Figure 6*A*). The effect on clonogenic growth was less pronounced because combined inhibition only sensitized cells to sirtinol (Supplemental Figure 4*B*, lower row). The strongest effect was observed in RKO in which co-treatment with 70 μM sirtinol and 20 μM PI3K inhibitor resulted in 50% reduced colony growth compared to LY294002 alone.

In contrast, in COLO 205 cells combined inhibition of NAMPT and PI3K reduced the rate of apoptotic cells compared to FK866 alone (Figure 6*B*). The clonogenic assay of these cells also revealed slight antagonistic action of the therapy combination at 5 nM FK866 (Figure 4*B*, lower row). Compared to the PI3K inhibitor alone, the combination FK866 and LY294002 also reduced the apoptotic fraction (20.3% to 14.8%; 27.2% to 22.3%) in HT29 and RKO, respectively (Figure 6*B*). Extended incubation for 2 weeks with the drug combination strongly interfered with growth inhibition as seen with FK866 alone in HT29 and RKO (Figure 4*B*, lower row).

Taken together, concomitant blocking NAMPT and PI3K activities resulted in antagonistic effects in the three *BRAF*-mutant CRC cell lines tested.

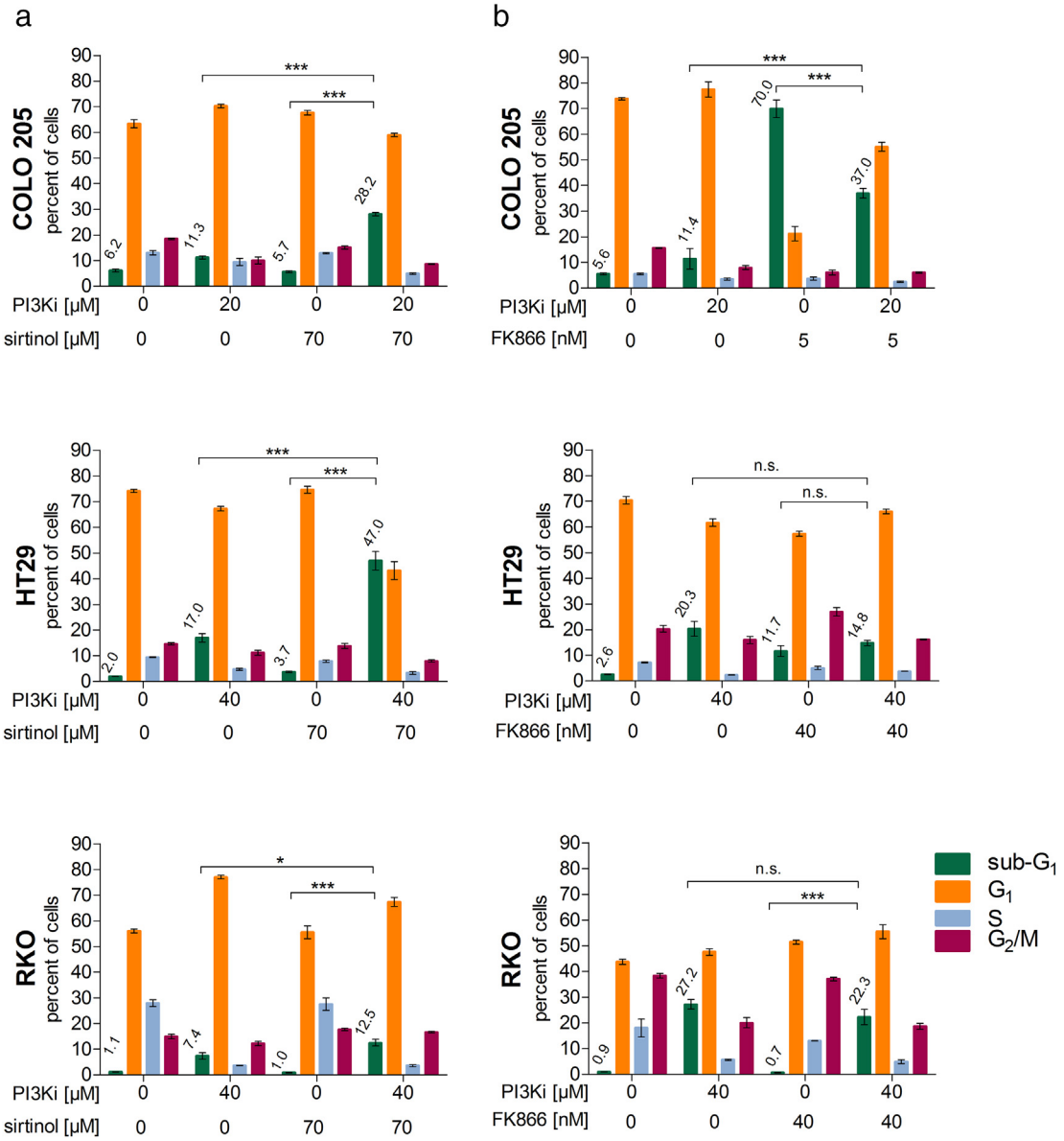

Figure 6. Combined inhibition of PI3K and SIRT1 reveals synergistic action while combining PI3K and NAMPT inhibitors has antagonistic effects in *BRAF*-mutant CRC cell lines.(a) DNA content analyses demonstrate effects of combined inhibition: Results of inhibition of PI3K, using LY294002, combined with SIRT1 inhibition by sirtinol analyzed 2 days after addition of drug, or solvent (0) to the indicated cell lines.(b) Results of the co-treatment with PI3K inhibitor and NAMPT inhibitor FK866 for 3 days are depicted.DNA content analyses with percentages of sub-G_1, G_1, S and G_2/M cell cycle phases of biological triplicates with standard deviation are given with percentage values of sub-G_1 fractions. Statistical analysis of one-way ANOVA followed by Tukey's post-hoc test. * $p < .05$, ** $p < .01$, *** $p < .001$.

Interfering with the c-MYC-NAMPT-DBC1-SIRT1 Positive Feedback Loop has a Dual Therapeutic Effect

SIRT1 is linked to c-MYC in a positive feedback loop that involves post-translational modifications affecting protein stability [10]. We therefore asked whether pharmacological targeting NAMPT or SIRT1 influences expression of factors of the loop and their downstream effectors. To assess the role of TP53 we used parental *BRAF*-mutant, *TP53* wild-type RKO (*TP53*$^{+/+}$) cells, and RKO (*TP53*$^{-/-}$) cells in which both alleles of *TP53* were deleted by targeted homologous recombination. Immunoblot analyses revealed lower c-MYC expression upon inhibition of SIRT1 by sirtinol, and upon inhibition of NAMPT by FK866, when compared to controls. These effects were more pronounced in RKO *TP53*$^{+/+}$ than in RKO *TP53*$^{-/-}$ cells (Figure 7*A*). SIRT1 protein levels were also lower in the presence of sirtinol (Figure 7*A*). We also assessed the expression of the cyclin dependent kinase inhibitor 1/ p21 protein. It served as a read-out for the activity of TP53, which induces p21 [29], and for the activity of c-MYC, which represses p21 [30–33].

In RKO *TP53*$^{+/+}$, we observed a temporary slight increase of p21 expression 48 hours after FK866 addition (Supplemental Figure 7*A*), that was almost absent at 72 hours (Supplemental Figure 7*B*). Elevated p21 expression corresponded to lower levels of c-MYC and of SIRT1, the negative regulator of TP53 (Figure 7, Supplemental

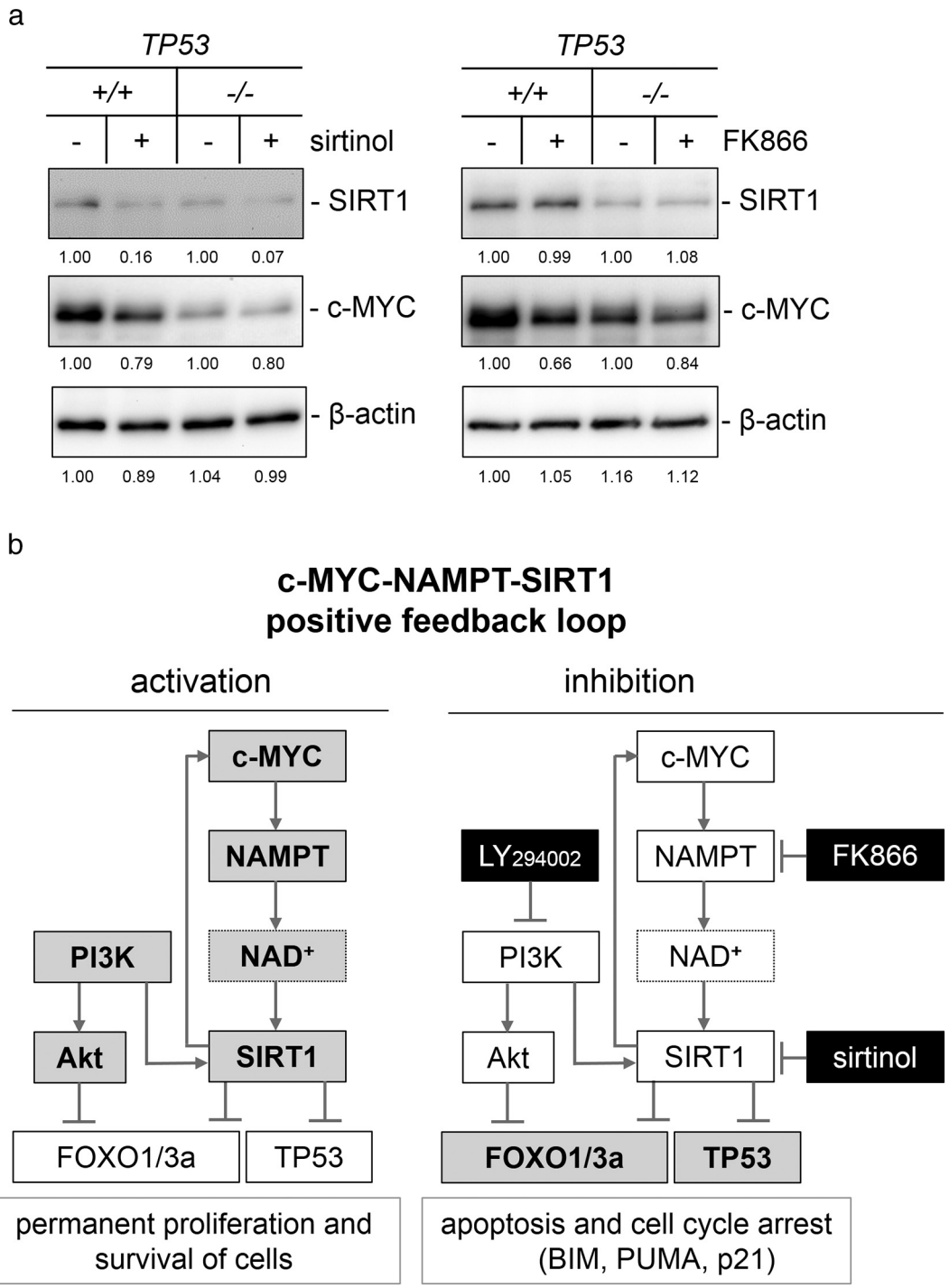

Figure 7. Molecular changes associated with pharmacological interference with the c-MYC-NAMPT-SIRT1 positive feedback loop in cancer cells(a) Immunoblot analysis of SIRT1, c-MYC and p21 expression in RKO *Tp53*$^{+/+}$ and RKO *Tp53*$^{-/-}$ CRC cells treated with sirtinol [30 μM] for 48 hours, or FK866 [5 nM] for 72 hours. The TP53 status of the cell lines was confirmed by immunoblot analysis (data not shown). β-actin served as loading control.(b) Model of the c-MYC-NAMPT-SIRT1 positive feedback loop in cancer cells and pathways affected by interference with pharmacological inhibitors.In cancer, deregulation of c-MYC leads to constitutive activation of the loop which contributes to permanent proliferation and survival of cells (see also author summary of [10]). Applying FK866 or sirtinol to inhibit NAMPT or SIRT1, respectively, disrupts the feedback loop and exerts a dual therapeutic effect, namely downregulation of c-MYC and de-repression of pro-apoptotic factors, such as TP53, and FOXO proteins. Both effects may contribute to growth arrest and cell death. Increased sensitivity to the drug combination of sirtinol and the PI3K inhibitor (LY294002) may be attributed to inactivation of SIRT1 by sirtinol together with the LY294002-mediated translocation of SIRT1 to the cytoplasm. Alleviation of SIRT1- and Akt-mediated FOXO protein repression may then lead to induction of apoptosis. Gray squares: activation, white squares: inhibition.

Figure 7*A*). In *TP53*$^{-/-}$ RKO, p21 expression slightly increased 72 hours after FK866 inoculation (Supplemental Figure 7*B*), which also correlated with reduced c-MYC levels (Figure 7*A*).

In contrast, sirtinol had no effect on p21 when analyzed 24, 48 (Supplemental Figure 7*C*), and 72 hours after drug administration (data not shown).

In summary, these data show, that pharmacological interference with NAMPT or SIRT1 activities represented a strategy to indirectly target the oncoprotein c-MYC, in both *TP53* wild-type and *TP53*-deficient *BRAF*-mutant CRC cells. Additionally, inhibition of NAMPT was associated with transient de-repression of TP53, which may have contributed to the capacity of FK866 to induce apoptosis, cell cycle arrest and abrogated colony growth.

Discussion

Up-Regulation of Feedback Loop Components in Murine Serrated Tumor Progression

Using *Braf*^{V637E} and *K-ras*^{G12Dint}/*Ink4a*/*Arf*$^{-/-}$ knock-in mouse models for serrated route CRC, we showed that in the proliferative zone of early mSH and in malignant progression of both mouse models c-MYC expression was high and correlated with up-regulation of SIRT1. Up-regulated c-MYC and SIRT1 associated with high NAMPT expression, which suggested that the positive feedback loop connecting the factors is active in murine serrated tumor progression. In agreement with our data, upregulation of c-MYC and downstream targets have previously been confirmed in these mouse models [8,9]. It is also in accordance with our previous findings of correlated high expression of c-MYC and SIRT1 in serrated route tumor progression [12] and with our data that showed elevated expression of c-MYC, NAMPT, and SIRT1 in human *BRAF* or *KRAS* serrated colorectal adenomas [14]. Together, these lines of evidence strongly suggested that oncogenic Braf and K-ras are directly associated with activation of the c-MYC-NAMPT-SIRT1 positive feedback loop in serrated route tumorigenesis. The expression of the feedback loop factors was not associated to the MSI status, WNT pathway activation, or TP53 pathway inactivation that are divergent in both mouse models.

By providing NAD^+, NAMPT contributes to activation of NAD^+-dependent SIRT1 [34]. We have demonstrated, that *NAMPT* is a direct transcriptional target of c-MYC and a necessary mediator for high SIRT1 levels in cancer cells [10]. Correlating with NAMPT induction, conditional activation of a c-MYC allele increases the NAD^+/NADH ratio [10]. Along these lines, a recent study showed elevated NAD^+/NADH ratios in large collections of cancer cell lines that corresponded to high NAMPT or other NAD^+ generating pathway activity [35]. Recently it was shown that increased NAD(H) in tumors caused by NAMPT activation promotes progression in the AOM/DSS colorectal cancer mouse model [36].

We showed that NAMPT was highly expressed in all epithelial cells in the small and large intestine of healthy control mice, corresponding to our observation of NAMPT expression in the normal human large intestine [14]. These findings strongly point to an essential role of NAMPT for intestinal epithelial cell physiology. High NAMPT activity explains why intestinal cells are able to have the highest (40× higher at maximum) NAD^+ production flux rate compared to other mouse tissues [37].

Interestingly, in the proliferative compartment of normal crypts and in the highly proliferating dysplastic/neoplastic cells in both mouse models, NAMPT was localized exclusively in the cytoplasm. In some differentiated villus epithelial cells, NAMPT was also localized in the nucleus. This supports that the subcellular distribution of NAMPT is associated with the proliferative state of the cell. Previous studies pointed to a cell cycle dependent regulation of NAMPT localization, with higher levels in the cytoplasm than in the nucleus in proliferating cells [38,39].

We detected high DBC1 expression in serrated lesions of *Braf* and *K-ras* mice. In normal cells the DBC1 protein binds to and inhibits SIRT1 [40]. However in cells with deregulated c-MYC, such as cancer cells, this function is impeded by c-MYC-mediated sequestration of DBC1, as we have shown [10]. In aggreement with this interaction of DBC1 and SIRT1 is absent, or weak in several tumor cell lines [41]. These studies suggest that deregulated c-MYC in serrated lesions may prevent DBC1-SIRT1 interactions and thus allow for hyperactive SIRT1 function, despite of high DBC1 expression.

Oncogenic mutations in either *K-ras* or *Braf* lead to constitutive activation of the MAPK/ERK1/2 pathway, contributing to post-translational regulation of c-MYC in serrated lesions [42]. In addition, in 50% of *Braf*^{V637E} mice high-grade dysplasia lesions and carcinomas, the Wnt pathway is activated during serrated tumorigenesis [9]. Since c-MYC is a transcriptional target of β-catenin/TCF4 [15], it may also contribute to the up-regulation of c-MYC and the feedback loop in serrated *Braf*^{V637E}-induced tumor progression. However, since all high-grade lesions and carcinomas displayed equally elevated protein expression, our IHC data did not reveal an association to WNT pathway activity.

Invasive carcinomas arise in a subset of the *Braf*^{V637E} mice with long latency. The two major tumor suppressive mechanisms in serrated lesions are apoptosis and oncogene-induced senescence [43]. The introduction of mutant *Tp53* in *Braf*^{V637E} knock-in mice, or inactivation of the CDK inhibitor *p16*^{Ink4a} in *Braf*^{V637E} and *K-Ras*^{G12D} mice significantly accelerate and enhance tumor progression and promote formation of additional metastases [8,9]. As SIRT1 prevents apoptosis and senescence by negatively regulating TP53 and other pro-apoptotic factors, in addition to promoting c-MYC activity [10], enhanced SIRT1 function in serrated lesions may therefore be of critical importance to antagonize the two mayor tumor suppressive mechanism and thus contribute to tumor progression. Initial studies of the mouse models also analyzed microsatellite stability. Of the Braf^{V637E}-induced mSA and carcinomas 39.4% were MSI-H and only 6% were MSS, whereas all Braf^{V637E}-induced hyperplastic polyps were MSS or MSI-L [9]. In contrast, the majority of murine K-ras-mutated tumors was either MSI-L (40%) or MSS (50%), and only 10% of the tumors were MSI-H [8]. Thus, the MSI status of tumors in both mouse models closely resembled the molecular characteristics of human BRAF or KRAS-mutated serrated polyps and carcinomas. The feedback loop components c-MYC, NAMPT, SIRT1 and DBC1 were consistently highly expressed in all lesions of both mouse models, suggesting that it is not directly linked to MSS or MSI status.

Targeting NAMPT is Efficacious as Monotherapy While Only Combination with a PI3K Inhibitor Sensitizes to Targeting SIRT1

In vitro and preclinical studies have demonstrated that the two enzymes of the feedback loop, NAMPT and SIRT1 represent potential cancer drug targets [44–48]. We recently screened public

pharmacogenomic databases to identify colorectal cancer cell lines with vulnerability to NAMPT and SIRT1 inhibitors [14]. The resulting cell lines all showed molecular signatures, such as *BRAF*, *RNF43* alterations, and microsatellite instability, which are characteristic features of serrated lesions.

In order to assess the kinetics and mechanism of drug action in *BRAF*-mutant CRC cell lines, we compared short- and long-term treatments using pharmacological NAMPT and SIRT1 inhibitors. NAMPT inhibition as monotherapy was highly effective in most cell lines when assessed 3 days after drug addition. Most notably, longer drug treatments of 2 weeks revealed additional efficacies of mono- and combination-therapy. Such delayed responses should be taken into account in future strategies evaluating NAMPT inhibitors.

Propagating cancer cells in three rather than two dimensions has been shown to create a reasonable heterogeneity at the cellular level with respect to proliferative capacity, hypoxic compartments, and Wnt and Notch signaling pathway activities which represent critical features of colorectal cancer stemness [49]. The preclinical model of tumoroids that reflect more natural organ conditions was highly sensitive to FK866. To our knowledge, this is the first study to show vulnerability of patient-derived, early passage CRC tumoroids towards NAMPT inhibition. It strongly supports NAMPT as a potential drug target in serrated CRC.

Although our previous analyses of pharmacogenomics databases revealed increased sensitivity of serrated route CRC cell lines compared to classical Wnt-driven cell lines, this was only observed when very high concentrations above 100 μM of a SIRT1 inhibitor (EX527) were tested [14]. The present study confirmed this, since all *BRAF*-mutant CRC cell lines and tumoroids were unresponsive to SIRT1 inhibition by sirtinol monotherapy in the low micromolar range. However, the combination of sirtinol and PI3K inhibitor slightly sensitized cells regardless of the mutational status of *PI3K* or *TP53.* An explanation for the sensitization to sirtinol may be that PI3K inhibition also affects SIRT1 function at multiple levels. First, PI3K inhibition leads to translocation of SIRT1 to the cytoplasm [50]. This abrogates cellular resistance to apoptosis which is mediated only by nuclear SIRT1 [51]. Second, since the PI3K pathway and SIRT1 both negatively regulate FOXO1 and FOXO3a functions, concomitant inhibition of SIRT1 and PI3K may converge on FOXO protein activation which leads to induction of apoptosis and cell cycle arrest (Figure 7*B*). Thus, such potential dual inhibition of SIRT1, together with the dual activation of FOXO proteins may explain the observed efficacy of combining inhibitors of SIRT1 and PI3K.

In contrast, co-inhibition of PI3K and NAMPT antagonized the effects of the NAMPT inhibitor. Tumor cells are extremely sensitive to NAMPT inhibition compared to normal cells, putatively due to their higher activity of NAD^+ consuming enzymes. FK866-mediated NAMPT inhibition leads to exhaustion of cytoplasmic and nuclear NAD^+, followed by ATP depletion, and either oncosis or autophagy and cell death [52]. Given that PI3K-mTOR inhibition robustly induces autophagy, by combining inhibition of NAMPT and PI3K, we expected to obtain additive or synergistic effects of excessive autophagic cell death. Surprisingly, co-inhibition of PI3K reduced the rate of cell death compared to FK866 monotherapy. A reason for this may be the high interconnection of PI3K with MAPK/ERK1/2 signaling pathways, with the intermediate metabolism network, and autophagy [53]. This leads to mutual feedback inhibition between MEK and PI3K signaling [23]. The close connection of the involved pathways has raised the speculation that inhibition of the PI3K-AKT–mTOR pathway may reduce sensitivity to metabolic inhibitors [23]. Although our results support this assumption, a detailed study of pharmacokinetics and mechanism of drug action will be necessary for the development of combination therapeutic strategies of SIRT1 and NAMPT inhibition.

High sensitivity to NAMPT monotherapy of all *BRAF*-mutant cell lines and tumoroids strongly indicated NAMPT as a potential new drug target for serrated route CRCs, including MSI and MSS types that have the worst prognosis. In agreement with previous observations [54], and our recent database analysis of CRC cell lines [14], vulnerability to FK866 inversely correlated with NAMPT protein expression. Therefore, NAMPT levels may serve as a predictive marker for therapy responsiveness. In future studies aiming to assess the translational significance in more detail, high FK866 sensitivity observed in the MSS cell lines HT29 and COLO 205 also needs to be confirmed with patient derived *BRAF*-mutant MSS tumor organoids and *in vivo* using patient-derived tumor xenografts.

Molecular Changes Following Interference with the c-MYC-NAMPT-DBC1-SIRT1 Circuitry

SIRT1 regulates c-MYC and TP53 by deacetylation. While the c-MYC protein becomes stabilized and activated [10], the transcriptional activity of TP53 is suppressed following SIRT1-mediated deacetylation [16,17]. In agreement with this positive feedback regulation that we previously established, we found that pharmacological inhibition of SIRT1 or NAMPT resulted in down-regulation of c-MYC. In addition, p21 levels slightly increased in $Tp53^{+/+}$ and also in $Tp53^{-/-}$ RKO cells upon inhibiting NAMPT by FK866. Since p21 is negatively regulated by c-MYC [30–33], the results indicated that besides TP53, which induces p21, also reduced c-MYC activity may have contributed to elevated p21 expression. Both effects, down-regulation of c-MYC and activation of TP53, are most likely the consequence of decreased SIRT1 function (Model: Figure 7*B*) [10,16,17] and explain apoptosis and growth arrest of CRC cell lines and tumoroids upon FK866 monotherapy.

Cytotoxicity of NAMPT or SIRT1 inhibition either involves activation [10,55,56], or has no effect on TP53 [48,57]. Cell line differences may be one reason for these discrepancies. According to our data in a genetic mouse model, TP53 plays an important role when feedback loop components are deregulated (Mohr et al., in preparation).

It was shown that NAMPT and SIRT1 inhibitors induce apoptosis in cancer stem cells which was in part attributed to de-repression of TP53 [58–62]. According to our data the interference with the c-MYC-NAMPT-DBC1-SIRT1 positive feedback loop additionally leads to down-regulation of c-MYC. In the future, preclinical analyses of NAMPT and SIRT1 inhibitors in $Braf^{V637E}$ and $K\text{-}ras^{G12Dint}$/$Ink4a/Arf^{-/-}$ mouse models, in patient-derived tumor xenograft (PDTX), or in patient-derived tumor organoid (PDTO) models will allow to determine the therapeutic impact of targeting the feedback loop components in serrated tumors *in vivo*. As simultaneous targeting of c-MYC and TP53 has recently been shown to eliminate cancer stem cells [63], interference with the loop may have the broader therapeutic potential not only to kill cancer cells, but more importantly in eliminating cancer stem cells.

These data together with our previous study [14] indicate, that NAMPT and SIRT1 may represent therapeutic targets in serrated B-Raf or Kras-driven, and also in WNT pathway driven colorectal cancers [46,64,65]. Future studies using preclinical models will have to address whether higher vulnerabilities of *BRAF*-mutant cell lines observed *in vitro* translates to similar findings *in vivo.*

Conclusions

Our data from two genetic mouse models support the oncogenic role of c-MYC/NAMPT/DBC1/SIRT1 positive feedback loop. Its direct association with the oncogenic drivers Braf and K-ras points to a contribution of the loop components to murine serrated route tumorigenesis.

Vulnerability to NAMPT inhibitor monotherapy or a combined PI3K/SIRT1 inhibitor strategy offered novel therapeutic opportunities for serrated CRCs. The dual therapeutic effect on c-MYC and TP53 has the potential for eliminating cancer stem cells. Our recent studies of entities with deregulated MYC proteins, such as basal cell carcinomas [13], and Wnt pathway-driven conventional CRC [14], as well as our unpublished work on pancreatic ductal adenocarcinomas and a mouse model of lymphomagenesis indicate that targeting the positive feedback loop represents an approach with potential broader applicability in other tumor types beyond *BRAF*-mutant CRCs. Since several NAMPT inhibitor regimens are currently tested also in cancer clinical trials [52,66], our findings may have rapid translational impact.

Acknowledgments

We thank Anja Heier for her expert support and excellent experimental assistance. We are grateful to Johannes Döbler for reading the manuscript and comments, help with graphics and software. We thank Bernhard Lüscher for reading the manuscript and comments. We are grateful to Oberdan Leo (Brussels) and Shin-ichiro Imai (Washington) for providing *Nampt*-floxed mice.

The study was funded by grants to A.M. by the German Research Foundation (DFG) [grant number Me1719/3-1], the German cancer aid [grant number 111483] and the German consortium for translational cancer research (DKTK).

Competing interests

On behalf of the authors I declare that there is no conflict of interest and all authors have read the journal's policy on conflicts of interest. A. Menssen.

Appendix A. Supplementary data

Supplementary data to this article can be found online at https://doi.org/10.1016/j.neo.2019.07.009.

References

[1] Rosty C, Hewett DG, Brown IS, Leggett BA, and Whitehall VL (2013). Serrated polyps of the large intestine: current understanding of diagnosis, pathogenesis, and clinical management. *J Gastroenterol* **48**, 287–302. https://doi.org/10.1007/s00535-012-0720-y.

[2] Snover DC (2011). Update on the serrated pathway to colorectal carcinoma. *Hum Pathol* **42**, 1–10. https://doi.org/10.1016/j.humpath.2010.06.002.

[3] Noffsinger AE (2009). Serrated polyps and colorectal cancer: new pathway to malignancy. *Annu Rev Pathol* **4**, 343–364. https://doi.org/10.1146/annurev.pathol.4.110807.092317.

[4] Ogino S, Nosho K, Kirkner GJ, Kawasaki T, Meyerhardt JA, Loda M, Giovannucci EL, and Fuchs CS (2009). CpG island methylator phenotype, microsatellite instability, BRAF mutation and clinical outcome in colon cancer. *Gut* **58**, 90–96. https://doi.org/10.1136/gut.2008.155473.

[5] Tol J, Nagtegaal ID, and Punt CJ (2009). BRAF mutation in metastatic colorectal cancer. *N Engl J Med* **361**, 98–99. https://doi.org/10.1056/NEJMc0904160.

[6] Samowitz WS, Sweeney C, Herrick J, Albertsen H, Levin TR, Murtaugh MA, Wolff RK, and Slattery ML (2005). Poor survival associated with the BRAF V600E mutation in microsatellite-stable colon cancers. *Cancer Res* **65**, 6063–6069. https://doi.org/10.1158/0008-5472.CAN-05-0404.

[7] Tran B, Kopetz S, Tie J, Gibbs P, Jiang ZQ, Lieu CH, Agarwal A, Maru DM, Sieber O, and Desai J (2011). Impact of BRAF mutation and microsatellite instability on the pattern of metastatic spread and prognosis in metastatic colorectal cancer. *Cancer* **117**, 4623–4632. https://doi.org/10.1002/cncr.26086.

[8] Bennecke M, Kriegl L, Bajbouj M, Retzlaff K, Robine S, Jung A, Arkan MC, Kirchner T, and Greten FR (2010). Ink4a/Arf and oncogene-induced senescence prevent tumor progression during alternative colorectal tumorigenesis. *Cancer Cell* **18**, 135–146. https://doi.org/10.1016/j.ccr.2010.06.013.

[9] Rad R, Cadinanos J, Rad L, Varela I, Strong A, Kriegl L, Constantino-Casas F, Eser S, Hieber M, and Seidler B, et al (2013). A genetic progression model of Braf(V600E)-induced intestinal tumorigenesis reveals targets for therapeutic intervention. *Cancer Cell* **24**, 15–29. https://doi.org/10.1016/j.ccr.2013.05.014.

[10] Menssen A, Hydbring P, Kapelle K, Vervoorts J, Diebold J, Luscher B, Larsson LG, and Hermeking H (2012). The c-MYC oncoprotein, the NAMPT enzyme, the SIRT1-inhibitor DBC1, and the SIRT1 deacetylase form a positive feedback loop. *Proc Natl Acad Sci U S A* **109**, E187-196. https://doi.org/10.1073/pnas.1105304109.

[11] Menssen A and Hermeking H (2012). c-MYC and SIRT1 locked in a vicious cycle. *Oncotarget* **3**, 112–113. https://doi.org/10.18632/oncotarget.440.

[12] Kriegl L, Vieth M, Kirchner T, and Menssen A (2012). Up-regulation of c-MYC and SIRT1 expression correlates with malignant transformation in the serrated route to colorectal cancer. *Oncotarget* **3**, 1182–1193. https://doi.org/10.18632/oncotarget.628.

[13] Brandl L, Hartmann D, Kirchner T, and Menssen A (2018). Expression of n-MYC, NAMPT and SIRT1 in basal cell carcinomas and their cells of origin. *Acta Derm Venereol* **99**, 63–71. https://doi.org/10.2340/00015555-3031.

[14] Brandl L, Kirstein N, Neumann J, Sendelhofert A, Vieth M, Kirchner T, and Menssen A (2018). The c-MYC/NAMPT/SIRT1 feedback loop is activated in early classical and serrated route colorectal cancer and represents a therapeutic target. *Med Oncol* **36**, 5. https://doi.org/10.1007/s12032-018-1225-1.

[15] He TC, Sparks AB, Rago C, Hermeking H, Zawel L, da Costa LT, Morin PJ, Vogelstein B, and Kinzler KW (1998). Identification of c-MYC as a target of the APC pathway. *Science* **281**, 1509–1512.

[16] Luo J, Nikolaev AY, Imai S, Chen D, Su F, Shiloh A, Guarente L, and Gu W (2001). Negative control of p53 by Sir2alpha promotes cell survival under stress. *Cell* **107**, 137–148.

[17] Vaziri H, Dessain SK, Ng Eaton E, Imai SI, Frye RA, Pandita TK, Guarente L, and Weinberg RA (2001). hSIR2(SIRT1) functions as an NAD-dependent p53 deacetylase. *Cell* **107**, 149–159.

[18] Chalkiadaki A and Guarente L (2015). The multifaceted functions of sirtuins in cancer. *Nat Rev Cancer* **15**, 608–624. https://doi.org/10.1038/nrc3985.

[19] Yoshino J, Baur JA, and Imai SI (2018). NAD(+) Intermediates: the biology and therapeutic potential of NMN and NR. *Cell Metab* **27**, 513–528. https://doi.org/10.1016/j.cmet.2017.11.002.

[20] Bonkowski MS and Sinclair DA (2016). Slowing ageing by design: the rise of NAD(+) and sirtuin-activating compounds. *Nat Rev Mol Cell Biol* **17**, 679–690. https://doi.org/10.1038/nrm.2016.93.

[21] Dollerup OL, Christensen B, Svart M, Schmidt MS, Sulek K, Ringgaard S, Stodkilde-Jorgensen H, Moller N, Brenner C, and Treebak JT, et al (2018). A randomized placebo-controlled clinical trial of nicotinamide riboside in obese men: safety, insulin-sensitivity, and lipid-mobilizing effects. *Am J Clin Nutr* **108**, 343–353. https://doi.org/10.1093/ajcn/nqy132.

[22] Cancer Genome Atlas N (2012). Comprehensive molecular characterization of human colon and rectal cancer. *Nature* **487**, 330–337. https://doi.org/10.1038/nature11252.

[23] Fruman DA and Rommel C (2014). PI3K and cancer: lessons, challenges and opportunities. *Nat Rev Drug Discov* **13**, 140–156. https://doi.org/10.1038/nrd4204.

[24] Medico E, Russo M, Picco G, Cancelliere C, Valtorta E, Corti G, Buscarino M, Isella C, Lamba S, and Martinoglio B, et al (2015). The molecular landscape of colorectal cancer cell lines unveils clinically actionable kinase targets. *Nat Commun* **6**, 7002. https://doi.org/10.1038/ncomms8002.

[25] Menssen A, Epanchintsev A, Lodygin D, Rezaei N, Jung P, Verdoodt B, Diebold J, and Hermeking H (2007). c-MYC delays prometaphase by direct transactivation of MAD2 and BubR1: identification of mechanisms underlying c-MYC-induced DNA damage and chromosomal instability. *Cell Cycle* **6**, 339–352. https://doi.org/10.4161/cc.6.3.3808.

[26] Sears RC (2004). The life cycle of C-myc: from synthesis to degradation *Cell Cycle* **3**. 1133–1137 DOI: 1145 [pii]; 2004.

[27] Neal JT and Kuo CJ (2016). Organoids as models for neoplastic transformation. *Annu Rev Pathol* **11**, 199–220. https://doi.org/10.1146/annurev-pathol-012615-044249.

[28] Bond CE, Umapathy A, Ramsnes I, Greco SA, Zhen Zhao Z, Mallitt KA, Buttenshaw RL, Montgomery GW, Leggett BA, and Whitehall VL (2012). p53 mutation is common in microsatellite stable, BRAF mutant colorectal cancers. *Int J Cancer* **130**, 1567–1576. https://doi.org/10.1002/ijc.26175.

[29] el-Deiry WS, Tokino T, Velculescu VE, Levy DB, Parsons R, Trent JM, Lin D, Mercer WE, Kinzler KW, and Vogelstein B (1993). WAF1, a potential mediator of p53 tumor suppression. *Cell* **75**, 817–825.

[30] Gartel AL, Ye X, Goufman E, Shianov P, Hay N, Najmabadi F, and Tyner AL (2001). Myc represses the p21(WAF1/CIP1) promoter and interacts with Sp1/Sp3. *Proc Natl Acad Sci U S A* **98**, 4510–4515. https://doi.org/10.1073/pnas.081074898.

[31] Herold S, Wanzel M, Beuger V, Frohme C, Beul D, Hillukkala T, Syvaoja J, Saluz HP, Haenel F, and Eilers M (2002). Negative regulation of the mammalian UV response by Myc through association with Miz-1. *Mol Cell* **10**, 509–521.

[32] Jung P, Menssen A, Mayr D, and Hermeking H (2008). AP4 encodes a c-MYC-inducible repressor of p21. *Proc Natl Acad Sci U S A* **105**, 15046–15051. https://doi.org/10.1073/pnas.0801773105.

[33] Seoane J, Le HV, and Massague J (2002). Myc suppression of the p21(Cip1) Cdk inhibitor influences the outcome of the p53 response to DNA damage. *Nature* **419**, 729–734. https://doi.org/10.1038/nature01119.

[34] Revollo JR, Grimm AA, and Imai S (2004). The NAD biosynthesis pathway mediated by nicotinamide phosphoribosyltransferase regulates Sir2 activity in mammalian cells. *J Biol Chem* **279**, 50754–50763. https://doi.org/10.1074/jbc.M408388200.

[35] Chowdhry S, Zanca C, Rajkumar U, Koga T, Diao Y, Raviram R, Liu F, Turner K, Yang H, and Brunk E, et al (2019). NAD metabolic dependency in cancer is shaped by gene amplification and enhancer remodelling. *Nature* . https://doi.org/10.1038/s41586-019-1150-2.

[36] Hong SM, Hwang SW, Wang T, Park CW, Ryu YM, Jung JH, Shin JH, Kim SY, Lee JL, and Kim CW, et al (2019). Increased nicotinamide adenine dinucleotide pool promotes colon cancer progression by suppressing reactive oxygen species level. *Cancer Sci* **110**, 629–638. https://doi.org/10.1111/cas.13886.

[37] Liu L, Su X, Quinn 3rd WJ, Hui S, Krukenberg K, Frederick DW, Redpath P, Zhan L, Chellappa K, and White E, et al (2018). Quantitative analysis of NAD synthesis-breakdown fluxes. *Cell Metab* **27**, 1067–1080. https://doi.org/10.1016/j.cmet.2018.03.018 e1065.

[38] Romacho T, Villalobos LA, Cercas E, Carraro R, Sánchez-Ferrer CF, and Peiró C (2013). Visfatin as a novel mediator released by inflamed human endothelial cells. *PLOS ONE* **8**e78283. https://doi.org/10.1371/journal.pone.0078283.

[39] Kitani T and Okuno S (2003). Fujisawa H. *Growth phase-dependent changes in the subcellular localization of pre-B-cell colony-enhancing factor FEBS Lett* **544**, 74–78 DOI: S0014579303004769 [pii].

[40] Kim JE, Chen J, and Lou Z (2008). DBC1 is a negative regulator of SIRT1. *Nature* **451**, 583–586. https://doi.org/10.1038/nature06500.

[41] Kim JE, Lou Z, and Chen J (2009). Interactions between DBC1 and SIRT 1 are deregulated in breast cancer cells. *Cell Cycle* **8**, 3784–3785. https://doi.org/10.4161/cc.8.22.10055.

[42] Sears R, Leone G, and DeGregori J (1999). Nevins JR. *Ras enhances Myc protein stability Mol Cell* **3**, 169–179 DOI: S1097-2765(00)80308-1 [pii].

[43] Kriegl L, Neumann J, Vieth M, Greten FR, Reu S, Jung A, and Kirchner T (2011). Up and downregulation of p16(Ink4a) expression in BRAF-mutated polyps/adenomas indicates a senescence barrier in the serrated route to colon cancer. *Mod Pathol* **24**, 1015–1022. https://doi.org/10.1038/modpathol.2011.43.

[44] Demarest TGMB, Okur MN, Dan X, Croteau DL, Fakouri NB, Mattson MP, and Bohr VA (2019). *NAD+ Metabolism in Aging and Cancer Annual Review of Cancer Biology* **3**, 1–26. https://doi.org/10.1146/annurev-cancerbio-030518-055905.

[45] Lain S, Hollick JJ, Campbell J, Staples OD, Higgins M, Aoubala M, McCarthy A, Appleyard V, Murray KE, and Baker L, et al (2008). Discovery, in vivo activity, and mechanism of action of a small-molecule p53 activator. *Cancer Cell* **13**, 454–463. https://doi.org/10.1016/j.ccr.2008.03.004.

[46] Zhang Q, Zeng SX, Zhang Y, Ding D, Ye Q, Meroueh SO, and Lu H (2012). A small molecule Inauhzin inhibits SIRT1 activity and suppresses tumour growth through activation of p53. *EMBO Mol Med* **4**(4), 298–312. https://doi.org/10.1002/emmm.201100211.

[47] Heltweg B, Gatbonton T, Schuler AD, Posakony J, Li H, Goehle S, Kollipara R, Depinho RA, Gu Y, and Simon JA, et al (2006). Antitumor activity of a small-molecule inhibitor of human silent information regulator 2 enzymes. *Cancer Res* **66**, 4368–4377. https://doi.org/10.1158/0008-5472.CAN-05-3617.

[48] Ota H, Tokunaga E, Chang K, Hikasa M, Iijima K, Eto M, Kozaki K, Akishita M, Ouchi Y, and Kaneki M (2006). Sirt1 inhibitor, Sirtinol, induces senescence-like growth arrest with attenuated Ras-MAPK signaling in human cancer cells. *Oncogene* **25**, 176–185. https://doi.org/10.1038/sj.onc.1209049.

[49] Schutte M, Risch T, Abdavi-Azar N, Boehnke K, Schumacher D, Keil M, Yildiriman R, Jandrasits C, Borodina T, and Amstislavskiy V, et al (2017). Molecular dissection of colorectal cancer in pre-clinical models identifies biomarkers predicting sensitivity to EGFR inhibitors. *Nat Commun* **8**14262. https://doi.org/10.1038/ncomms14262.

[50] Koga T, Suico MA, Shimasaki S, Watanabe E, Kai Y, Koyama K, Omachi K, Morino-Koga S, Sato T, and Shuto T, et al (2015). Endoplasmic reticulum (ER) stress induces sirtuin 1 (SIRT1) expression via the PI3K-Akt-GSK3beta signaling pathway and promotes hepatocellular injury. *J Biol Chem* **290**, 30366–30374. https://doi.org/10.1074/jbc.M115.664169.

[51] Tanno M, Sakamoto J, Miura T, Shimamoto K, and Horio Y (2007). Nucleocytoplasmic shuttling of the NAD+-dependent histone deacetylase SIRT1. *J Biol Chem* **282**, 6823–6832. https://doi.org/10.1074/jbc.M609554200.

[52] Sampath D, Zabka TS, Misner DL, O'Brien T, and Dragovich PS (2015). Inhibition of nicotinamide phosphoribosyltransferase (NAMPT) as a therapeutic strategy in cancer. *Pharmacol Ther* **151**, 16–31. https://doi.org/10.1016/j.pharmthera.2015.02.004.

[53] Shanware NP, Bray K, and Abraham RT (2013). The PI3K, metabolic, and autophagy networks: interactive partners in cellular health and disease. *Annu Rev Pharmacol Toxicol* **53**, 89–106. https://doi.org/10.1146/annurev-pharmtox-010611-134717.

[54] Xiao Y, Elkins K, Durieux JK, Lee L, Oeh J, Yang LX, Liang X, DelNagro C, Tremayne J, and Kwong M, et al (2013). Dependence of tumor cell lines and patient-derived tumors on the NAD salvage pathway renders them sensitive to NAMPT inhibition with GNE-618. *Neoplasia* **15**, 1151–1160.

[55] Thakur BK, Dittrich T, Chandra P, Becker A, Kuehnau W, Klusmann JH, Reinhardt D, and Welte K (2013). Involvement of p53 in the cytotoxic activity of the NAMPT inhibitor FK866 in myeloid leukemic cells. *Int J Cancer* **132**, 766–774. https://doi.org/10.1002/ijc.27726.

[56] Thakur BK, Dittrich T, Chandra P, Becker A, Lippka Y, Selvakumar D, Klusmann JH, Reinhardt D, and Welte K (2012). Inhibition of NAMPT pathway by FK866 activates the function of p53 in HEK293T cells. *Biochem Biophys Res Commun* **424**, 371–377. https://doi.org/10.1016/j.bbrc.2012.06.075.

[57] Gehrke I, Bouchard ED, Beiggi S, Poeppl AG, Johnston JB, Gibson SB, and Banerji V (2014). On-target effect of FK866, a nicotinamide phosphoribosyl transferase inhibitor, by apoptosis-mediated death in chronic lymphocytic leukemia cells. *Clin Cancer Res* **20**, 4861–4872. https://doi.org/10.1158/1078-0432.ccr-14-0624.

[58] Lucena-Cacace A, Otero-Albiol D, Jimenez-Garcia MP, Munoz-Galvan S, and Carnero A (2018). NAMPT is a potent oncogene in colon cancer progression that modulates cancer stem cell properties and resistance to therapy through Sirt1 and PARP. *Clin Cancer Res* **24**, 1202–1215. https://doi.org/10.1158/1078-0432.CCR-17-2575.

[59] Lucena-Cacace A, Otero-Albiol D, Jimenez-Garcia MP, Peinado-Serrano J, and Carnero A (2017). NAMPT overexpression induces cancer stemness and defines a novel tumor signature for glioma prognosis. *Oncotarget* **8**, 99514–99530. https://doi.org/10.18632/oncotarget.20577.

[60] Lee JS, Park JR, Kwon OS, Lee TH, Nakano I, Miyoshi H, Chun KH, Park MJ, Lee HJ, and Kim SU, et al (2015). SIRT1 is required for oncogenic

transformation of neural stem cells and for the survival of "cancer cells with neural stemness" in a p53-dependent manner. *Neuro Oncol* **17**, 95–106. https://doi.org/10.1093/neuonc/nou145.

[61] Li L, Osdal T, Ho Y, Chun S, McDonald T, Agarwal P, Lin A, Chu S, Qi J, and Li L, et al (2014). SIRT1 activation by a c-MYC oncogenic network promotes the maintenance and drug resistance of human FLT3-ITD acute myeloid leukemia stem cells. *Cell Stem Cell* **15**, 431–446. https://doi.org/10.1016/j.stem.2014.08.001.

[62] Li L, Wang L, Li L, Wang Z, Ho Y, McDonald T, Holyoake TL, Chen W, and Bhatia R (2012). Activation of p53 by SIRT1 inhibition enhances elimination of CML leukemia stem cells in combination with imatinib. *Cancer Cell* **21**, 266–281. https://doi.org/10.1016/j.ccr.2011.12.020.

[63] Abraham SA, Hopcroft LE, Carrick E, Drotar ME, Dunn K, Williamson AJ, Korfi K, Baquero P, Park LE, and Scott MT, et al (2016). Dual targeting of p53 and c-MYC selectively eliminates leukaemic stem cells. *Nature* **534**, 341–346. https://doi.org/10.1038/nature18288.

[64] Lv X, Zhang L, Zhu Y, Said HM, Shi J, and Xu G (2015). Regulative effect of Nampt on tumor progression and cell viability in human colorectal cancer. *J Cancer* **6**, 849–858. https://doi.org/10.7150/jca.12341.

[65] Ueno T, Endo S, Saito R, Hirose M, Hirai S, Suzuki H, Yamato K, and Hyodo I (2014). The sirtuin inhibitor tenovin-6 upregulates death receptor 5 and enhances cytotoxic effects of 5-fluorouracil and oxaliplatin in colon cancer cells. *Oncol Res* **21**, 155–164. https://doi.org/10.3727/096504013X13854886566598.

[66] Karpov AS, Abrams T, Clark S, Raikar A, D'Alessio JA, Dillon MP, Gesner TG, Jones D, Lacaud M, and Mallet W, et al (2018). Nicotinamide phosphoribosyltransferase inhibitor as a novel payload for antibody-drug conjugates. *ACS Med Chem Lett* **9**, 838–842. https://doi.org/10.1021/acsmedchemlett.8b00254.